Temperature Dependence of Equilibrium and Rate Constants of Reactions Inducing Conversion between Hydrated Electron and Atomic Hydrogen

ARTICLE *in* THE JOURNAL OF PHYSICAL CHEMISTRY · MAY 1994

Impact Factor: 2.78 · DOI: 10.1021/j100070a037

3 AUTHORS, INCLUDING:

Geni Rina Sunaryo
Badan Tenaga Nuklir Nasional
11 PUBLICATIONS **172** CITATIONS

Temperature Dependence of Equilibrium and Rate Constants of Reactions Inducing Conversion between Hydrated Electron and Atomic Hydrogen

Hirotsugu Shiraishi*

Department of Chemistry and Fuel Research, Japan Atomic Energy Research Institute, Tokai-mura, Naka-gun, Ibaraki-ken 319-11, Japan

Geni R. Sunaryo and Kenkichi Ishigure

Department of Quantum Engineering and Systems Science, University of Tokyo, 7-3-1 Hongo, Bunkyo-ku, Tokyo 113, Japan

Received: November 17, 1993; In Final Form: February 22, 1994®

Pulse radiolysis experiments were performed on two equilibrium reactions, $e^-_{aq} + H^+ \rightleftharpoons H$ (1) and $e^-_{aq} + NH_4^+ \rightleftharpoons H + NH_3$ (5), in aqueous solution in a range between 25 and 250 °C. Equilibrium 1 was observed at temperatures above 100 °C, where dissociation of H becomes rapid, while equilibrium 5, which had been studied by Schwarz below 100 °C, was observed in the whole temperature range. The two sets of measurements gave consistent results. $pK_a(H)$ was found to decrease from 9.59 ± 0.03 at 25 °C to 6.24 ± 0.09 at 250 °C, while its van't Hoff plot curved concave upward to show that $\Delta C_p°(1)$ becomes increasingly more positive above 100 °C. The curvature is qualitatively as expected from decrease in the stability of ionic species with reduction in the dielectric constant of water. $C_p°(e^-_{aq})$ at 25 °C was estimated to be -4 ± 11 cal K^{-1} mol^{-1}, which is large as an anion, probably because of loose solvation structure of e^-_{aq}. Arrhenius plots of rate constants k_1 and k_5 both showed significant concave upward curvature in a region corresponding to temperature above 150 °C, while those of k_{-1} and k_{-5} did concave downward curvature in the same region. The reducing dielectric constant is presumed substantially to influence these features.

Introduction

In the field of water chemistry of nuclear reactors much attention has recently been paid to radiolysis of cooling water in the primary circuit.[1-3] With respect to the boiling-water reactor, in particular, plant tests have been carried out to examine the efficiency of hydrogen injection in diminishing oxidizing radiolytic products, O_2 and H_2O_2.[3] Concurrently a number of basic studies have been performed to provide experimental data on the temperature dependence of relevant rate constants[4-7] and G values.[8-12]

The aim of the present study was to investigate equilibrium constant K_1 and rate constants k_1 and k_{-1} of reaction 1 at high temperature:

$$e^-_{aq} + H^+ \rightleftharpoons H \qquad (1)$$

K_1 is related to equilibrium constant K_2 of reaction 2 through eq 3:

$$e^-_{aq} + H_2O \rightleftharpoons H + OH^- \qquad (2)$$

$$K_2 = K_1K_W \qquad (3)$$

where K_W is the ionic product for dissociation of water:

$$H_2O \rightleftharpoons H^+ + OH^- \qquad (4)$$

Although rapid recombination of e^-_{aq} and H had precluded observation of the attainment of equilibrium 1 or 2, rate constants k_2 and k_{-2} had been measured separately, and the results had led to an estimation for $pK_a(H)$ being about 9.6 at 25 °C.[13] Activation energies for k_2 and k_{-2} below 100 °C had also been reported by Fielden and Hart[14] and by Hickel and Sehested,[15] respectively. Though not generally recognized, it was possible to predict from these data and the temperature dependence of K_W that k_{-1} would increase with temperature much more rapidly than k_1. That is to say, large decrease of K_1 and fast equilibration in a nearly neutral solution could be expected for high-temperature conditions. Since reactivity of e^-_{aq} is different from that of H in some reactions, such change was presumed to have significant influence in the kinetics of radiolysis at high temperature. However, it was not certain whether the reported activation energies for k_2 and k_{-2} might be used for extensive extrapolation beyond 100 °C. On the other hand, though literature data for k_1 below 100 °C suggested that the temperature dependence of reaction 1 is not much different from that of a diffusion-controlled reaction, no experimental data had been reported for k_1 at high temperature, nor had been any attempt to measure k_{-1}.

It was found in an early series of the present experiments that e^-_{aq} produced pulse-radiolytically in dilute aqueous solution of perchloric acid decreased in two steps at temperatures above 100 °C, a slowly decreasing component being more pronounced at higher temperatures. Confirmation was made that the first step represented approach to an equilibrium concentration of e^-_{aq}, while the second step did slow decay of e^-_{aq} due to recombination reactions. Experiments were then performed up to 250 °C to evaluate k_1, k_{-1}, and K_1, and the results were reported briefly at a symposium.[16]

However, reexamination was later found necessary, when Schwarz published a pulse-radiolysis study on equilibrium 5:[17]

$$e^-_{aq} + NH_4^+ \rightleftharpoons H + NH_3 \qquad (5)$$

An advantage of this method is that the rate of equilibration can be enhanced in a pH range suitable for observing the equilibrium. From the measurement on K_5 between 5 and 85 °C, Schwarz evaluated K_2 by use of K_6 for

$$NH_3 + H_2O \rightleftharpoons NH_4^+ + OH^- \qquad (6)$$

Thermodynamic properties of e^-_{aq} were then derived to revise

® Abstract published in *Advance ACS Abstracts*, April 1, 1994.

0022-3654/94/2098-5164$04.50/0

earlier estimates.[17,18] He also pointed out that our data for K_1 around 200 °C, cited as a private communication, are in reasonable agreement with values predicted from his data. However, considerable discrepancy existed below 200 °C, where errors in our data were large because of very small absorbance in the second step. In view of the importance of equilibrium 1, it was decided for us to perform experiments on the NH_4^+/NH_3 system up to 250 °C. Simultaneously, examination was made on the earlier experiments, which turned out to have contained two problems leading to underestimation of K_1, one in the apparatus and another in the method of analysis. Hence, additional experiment on the $HClO_4$ system was carried out as well as reanalysis of the earlier data.

Other related studies were reported shortly before and during the present investigation. Rate constant k_1 was measured up to 200 °C by Elliot et al.[19] Examination on the temperature dependence of k_{-2} below 100 °C was made by Han and Bartels,[20] who obtained an activation energy larger than the value of Hickel and Sehested by 2.9 kcal mol^{-1}. Further, Schwarz[21] reinvestigated the temperature dependence of k_2 to correct the earlier activation energy by Fielden and Hart. Research on the temperature dependence of the initial G values was also advanced.[12,22] The results of these recent studies were referred to in the analysis of the present study. In the following, detailed description is given about the whole series of our experiments on equilibria 1 and 5. An experiment directly aiming at observing equilibrium 2 was not undertaken, since difficulty was presumed in maintaining concentration of dilute alkali at high temperature.

Experimental Section

The apparatus for the pulse-radiolysis experiments on high-temperature water is similar to the one used by Buxton et al.[25] in that a flow-type optical cell and a syringe reservoir are both set inside a steel pressure vessel. An electron-beam window of the vessel was a 50-μm-thick titanium foil, which was backed up by a grid with open area of 60%. Optical windows were quartz plates of 9 mm in thickness. The vessel was pressurized with He to a pressure about 0.5 MPa above the vapor pressure of water.

The optical cell, 1 cm in optical path length and 5 mm in depth, was covered by an aluminum heater block which had a hole of 14 mm in diameter and a pair of slits, 3 mm in width, to let pass an electron beam and analyzing light, respectively. The block was thermostatted to ±1 °C and sample temperature was monitored with a thermocouple inserted into the cell. The syringe, 100 cm^3 in volume, was made of quartz to avoid dissolution of alkali. To prevent convection the flow line was made from capillary tube, but no Teflon joint was used upstream to the optical cell to inhibit intrusion of oxygen. Sample was refreshed after every two or three shots of pulses by opening a remote-controlled valve in the flow line. In an experiment on H_2 solution a magnetic stirrer was attached to the syringe to accelerate the dissolution.

The pulse radiolysis was performed with a Dynamitron accelerator in the Research Center for Nuclear Science and Technology of the University of Tokyo. It produced a 0.1- or 0.2-μs electron beam at 2.2 MV to deliver a dose from 0.4 to 1.6 Gy/pulse at the optical cell. Individual pulse dose was monitored by a current incident on the heater block, but the accuracy was not very good, ±10%, due probably to insensitivity to beam shape. A 300-W Xe lamp was used for the analyzing light, and most measurements were made at 824 nm, where the lamp emits intense resonance lines. (The absorption maximum of e_{aq}^- shifts from 720 nm at 25 °C to about 1000 nm at 250 °C.[23,24]) The first-order response time of the detection system, including a PIN photodiode, amplifiers and a transient-waveform recorder, was 40 ns. It was found that in the initial series of experiments a backoff circuit in the detection system had caused baseline shift of an order of 10^{-5} in absorbance to lead to underestimation of K_1. The circuit was later improved, and appropriate correction was applied to the earlier data.

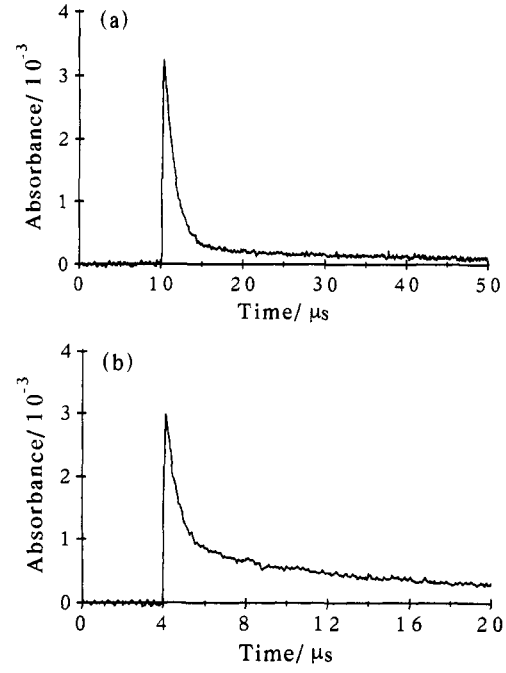

Figure 1. Time profiles of e_{aq}^- absorption observed at 200 °C, showing two-stepped decay: (a) 2.5 × 10^{-6} m in [$HClO_4$]; (b) 5 × 10^{-3} m in [NH_4Cl] and 6.7 × 10^{-3} m in [NH_3]. The measurements were made at 824 nm and with a 0.1-μs electron pulse delivering a dose of about 0.8 Gy. The second-step decay in (b) is partly due to impurity.

Water was purified with a Mili-Q filtration system. Perchloric acid of G.R. grade was used for the experiments on reaction 1. Since slight alkaline dissolution seemed to have occurred during preparation with Pyrex flasks, H^+ concentration was estimated from an observed decay rate of e_{aq}^- at 25 °C, and k_1 was taken to be 2.3 × 10^{10} dm^3 mol^{-1} s^{-1}.[25] Solutions were deaerated by bubbling with Ar gas.

Concentrated aqueous ammonia and aqueous hydrochloric acid, both of G.R. grade, were used for the experiments on reaction 5 after purification by isothermal distillation. Since Ar bubbling caused some loss of dissolved ammonia, its concentration was measured after bubbling by potentiometric titration with an HCl solution. In the present experimental conditions [NH_4^+] was virtually equal to [Cl^-]. Preliminary measurements on NH_4^+/NH_3 solutions at high temperatures suffered from an impurity effect, which turned out to be due mostly to dissolved carbon dioxide that might change from unreactive HCO_3^- to reactive CO_2. Preparative procedures were then improved to avoid its dissolution. However, there still remained a small amount of impurity, which caused complication in the data analysis.

Results and Discussion

First, the results on the two experimental systems are outlined with emphasis on initial confirmative measurements. The method of data analysis is explained next, and then the estimated equilibrium constants and rate constants are described with some discussion. Unless otherwise noted, the molal units, based on m, i.e., mol kg^{-1}, are used for equilibrium constants, but rate constants are expressed in the molar units.

Figure 1a illustrates an example of a time profile for e_{aq}^- absorption observed with 2.5 × 10^{-6} m $HClO_4$ solution. As seen, there is a distinct slow component in this 200 °C datum. To confirm that the slow component is also ascribed to e_{aq}^-, wavelength dependence was examined at both 200 and 250 °C. The decay profiles measured at 750, 824, and 1000 nm were identical in shape. It was also found that the slow component diminished with an increase in [$HClO_4$] until at 1 × 10^{-4} m it was hardly observable even at 250 °C.

Effect of two kinds of additives was examined with 6×10^{-6} m $HClO_4$ solution. One of them was ethanol, which is reactive toward H atom but is unreactive toward e_{aq}^-.[25] As expected, the slow component disappeared on addition of 5×10^{-2} m ethanol, whereas the first-step decay was little affected. The other additive was H_2, which converts OH to H through reaction 7. The initial

$$OH + H_2 \rightarrow H + H_2O \qquad (7)$$

yield of OH is reported to increase with temperature somewhat more than that of e_{aq}^-.[10,12] It was confirmed that addition of H_2 in concentration of 1×10^{-2} m resulted in approximate doubling of the slow component at high temperatures, though at this $[H_2]$ the conversion of OH was not so fast as to be regarded instantaneous.

Thus, all the observations consistently pointed to equilibrium between e_{aq}^- and H, and since the equilibration rate tended to increase with $[H^+]$, the dominant path was considered not to be reaction 2 but to be reaction 1. Detailed measurements were then carried out by using $HClO_4$ solution in a range between 2.5×10^{-6} and 1.1×10^{-5} m. At each temperature and concentration, pulse dose was varied in three steps, 0.4, 0.8, and 1.6 Gy, so that correction about recombination reactions could be made by use of the dose dependence of decay curves.

The experiments on the NH_4^+/NH_3 system were performed mainly above 100 °C. The concentration of NH_4^+, viz., $[NH_4Cl]$, was either 5×10^{-3} or 0.1 m, and measurements were made at two $[NH_3]/[NH_4^+]$ ratios, about 0.75 and 1.3. The pH decreased with temperature due to changes in K_6[26] and in K_W.[27] For instance, pH of a solution containing 5×10^{-3} m NH_4^+ and 6.7×10^{-3} m NH_3, was 9.4 at 25 °C, while it was estimated to be 6.0 and 5.3, respectively, at 200 and 250 °C.

A typical two-stepped profile observed with a solution containing 5×10^{-3} m NH_4^+ and 6.7×10^{-3} m NH_3 is shown in Figure 1b. It is seen that both the equilibration rate and the second-step absorbance are larger than in Figure 1a. In the experiments on NH_4^+/NH_3 solutions, pulse dose was varied only in two steps, 0.4 and 0.8 Gy, since recombination reactions were less disturbing than in $HClO_4$ solutions. There was, however, a problem about impurity.

The aim of the experiments at 0.1 m in $[NH_4^+]$ was to make the rate of equilibration much larger than that of radical recombination, so that the second-step absorbance could unambiguously extrapolated to time zero. A disadvantage was that above 100 °C the first-step decay was too fast to be measured accurately, and hence, initial $[e_{aq}^-]$ had to be estimated indirectly.

Method of Data Analysis. $HClO_4$ Solution. In the present system, $[e_{aq}^-]$ should, ideally, approach exponentially to an equilibrium value. But in practice, use of extremely small pulse dose was impossible because of a poor S/N ratio. Since there was little indication of impurity in $HClO_4$ solutions, a main point of the analysis was to correct for the dose effect due to recombination with radicals and pulse-produced H^+.

Since exact temperature dependence is unknown for some of the involved recombination reactions, an assumption was made that every pair of radicals reacts with the same rate constant, k_R. The kinetics can then be expressed approximately as

$$d[e_{aq}^-]/dt = -k_1[e_{aq}^-][H^+] + k_{-1}[H] - k_2[e_{aq}^-] + k_{-2}[OH^-][H] - k_R[e_{aq}^-][R] \qquad (8a)$$

$$d[H]/dt = k_1[e_{aq}^-][H^+] - k_{-1}[H] + k_2[e_{aq}^-] - k_{-2}[OH^-][H] - k_R[H][R] \qquad (8b)$$

$$d[R]/dt = -k_R[R]^2 \qquad (8c)$$

where [R] stands for a total radical concentration, $[e_{aq}^-] + [H] + [OH]$. An effect of pulse-produced H_2O_2 is ignored here. The terms for reaction 2, $k_2[e_{aq}^-]$ and $k_{-2}[OH^-][H]$, had been neglected in the earlier analysis,[16] but it was realized later that these are not necessarily negligible at high temperatures.

In the present dilute conditions, $[H^+]$ cannot be regarded to be constant with time, since $[e_{aq}^-]$ is not negligible in an equality $[H^+] = [ClO_4^-] + [e_{aq}^-] + [OH^-]$. For simplicity, $[OH^-]$ was assumed to be constant, and the variation of $[H^+]$ was approximated as

$$[H^+] = [H^+]_0 + [e_{aq}^-]_i \exp\{-(k_{eq} + k_R[R]_i)t\} \qquad (9)$$

$$[H^+]_0 = [ClO_4^-] + [OH^-]_0$$

$$k_{eq} = k_1[H^+]_0 + k_{-1} + k_2 + k_{-2}[OH^-]_0$$

where the suffixes 0 and i signify, respectively, concentration before pulsing and that immediately after pulsing, and $[OH^-]_0$ is calculable from literature data on K_W.[27] As defined, parameter k_{eq} is equal to the equilibration rate. Further, the first term of eq 8a and that of eq 8b were approximated as

$$k_1[e_{aq}^-][H^+] = k_1[e_{aq}^-][H^+]_0 + (1 + k_R[R]_i t)^{-1} k_1[e_{aq}^-]_i^2 \exp\{-(2k_{eq} + k_R[R]_i)t\} \qquad (10)$$

The rate equations can then be solved analytically to give

$$[e_{aq}^-] = (1 + k_R[R]_i t)^{-1} ([e_{aq}^-]_i + [H]_i)\{A \exp(-k_{eq}t) + B + C\} \qquad (11)$$

$$A = ([e_{aq}^-]_i + [H]_i)^{-1}[e_{aq}^-]_i\{1 - (k_{eq} + k_R[R]_i)^{-1}k_1[e_{aq}^-]_i\} - B$$

$$B = (k_1[H^+]_0 + k_{-1})^{-1}k_{-1} = (k_2 + k_{-2}[OH^-]_0)^{-1}k_{-2}[OH^-]_0$$

$$C = ([e_{aq}^-]_i + [H]_i)^{-1}(k_{eq} + k_R[R]_i)^{-1} \times k_1[e_{aq}^-]_i^2 \exp\{-(2k_{eq} + k_R[R]_i)t\}$$

From the definition, parameter B equals $[e_{aq}^-]_{eq}/([e_{aq}^-]_{eq} + [H]_{eq})$, where the suffix eq denotes an equilibrium value.

Not only the analysis on the data for $HClO_4$ solutions but also that for NH_4^+/NH_3 solutions require information on $[H]_i$. The ratio of the initial yields $G_H/G_{e_{aq}^-}$ is known to be 0.2 at 25 °C, but its temperature dependence had not been well established. Hence, a supplementary pulse-radiolysis experiment was performed on a solution containing 2×10^{-3} m NaOH and 0.1 m NH_3. A two-stepped rise in e_{aq}^- absorbance was observed, showing conversion from the spur-produced H atom to e_{aq}^-. The measurement was made only up to 200 °C to avoid deterioration of the quartz cell, but the data suggested that $G_H/G_{e_{aq}^-}$ changes little with temperature. Accordingly, $G_H/G_{e_{aq}^-}$ was assumed to be 0.2 irrespective of temperature. Quite recently, Elliot et al. have reported that $G_H/G_{e_{aq}^-}$ increases from 0.22 at 25 °C to 0.25 at 250 °C,[12] and Katsumura et al. have also observed a similar increase.[28] The neglect of the small temperature dependence does not introduce large error in the present analysis.

Actual procedures of the analysis were as follows. First, a simple first order analysis was made on each decay curve after subtracting appropriately assigned second step absorbance, and the calculated decay rate was plotted against pulse dose. An approximate value for k_{eq} was estimated from the intercept, while $k_R[R]_i$ was calculated from the slope with allowance for contribution from reaction between e_{aq}^- and pulse-produced H^+. To note the degree of the dose effect for a case of 5×10^{-6} m in $[ClO_4^-]$, a ratio of an apparent first order rate at the largest pulse dose, 1.6 Gy, to k_{eq} was about 1.4 up to 150 °C and then diminished

gradually to about 1.2 at 250 °C. $k_R[R]_i$ was found to change little with $[ClO_4^-]$.

To estimate k_{eq}, B, and $k_R[R]_i$ more accurately, a curve-fitting method based on eq 11 was then applied to all the data by using the above-obtained parameters as initial guess. Both the response time of the apparatus and the pulse width were taken into account, and the simulation was repeated until experimental curves for different pulse doses could be fitted with a consistent set of parameters. Generally, the result was satisfactory, though the fitting appeared imperfect for the data at the largest pulse dose, and some degree of uncertainty remained in both $k_R[R]_i$ and B.[29] No correction was made about the effect of ionic strength, since $[ClO_4^-]$ was at most 1.1×10^{-5} m in the analyzed data.

Method of Data Analysis. NH_4^+/NH_3 Solution. As mentioned already, there was an impurity problem in the NH_4^+/NH_3 system. Even after plausible correction for the effect of pulse dose, significant decay remained in the second step especially in the data at high temperatures. The corrected second step decay rate was not simply correlated either with $[NH_3]$ or $[NH_4^+]$, indicating that it is determined by impurity. Kinetic equations were, therefore, assumed as

$$d[e_{aq}^-]/dt = -k_5'[NH_4^+][e_{aq}^-] + k_{-5}[NH_3][H] - k_1'[e_{aq}^-][H^+] + k_{-1}[H] - k_2[e_{aq}^-] + k_{-2}[OH^-][H] - k_R[e_{aq}^-][R] - k_p[e_{aq}^-][P] \quad (12a)$$

$$d[H]/dt = k_5'[NH_4^+][e_{aq}^-] - k_{-5}[NH_3][H] + k_1'[e_{aq}^-] \times [H^+] - k_{-1}[H] + k_2[e_{aq}^-] - k_{-2}[OH^-][H] - k_R[H][R] \quad (12b)$$

$$d[R]/dt = -k_R[R]^2 \quad (12c)$$

Here, the terms for reactions 1 and 2 are included, since they contribute appreciably in the less concentrated solutions of 5×10^{-3} m in $[NH_4^+]$. k_5' and k_1' refer to rate constants at the employed ionic strength. Both k_{-5} and k_{-1} are assumed to be independent of ionic strength, and hence $K_5 = k_5/k_{-5} = k_5'/(\gamma^2 k_{-5})$, where γ is a mean activity coefficient for e_{aq}^- and NH_4^+. It is again assumed that every pair of radical reacts with the same rate constant k_R. Actually, the analysis showed that $k_R[R]_i$ was about half the one for the $HClO_4$ solution at the same temperature, most probably because OH is converted to less reactive NH_2.

The term $k_p[e_{aq}^-][P]$ represents an effect of impurity. The reason for the omission of the corresponding term for H atom is as follows. First, CO_2 is considered to be the most probable impurity. Second, an Arrhenius plot of the decay rate due to impurity, k_v in eq 13 below, showed a maximum around 175 °C. This behavior could readily be explained if the decay rate was assumed to be proportional to $[e_{aq}^-]_{eq}/([e_{aq}^-]_{eq} + [H]_{eq})$ which reduces with temperature.

In eq 12 $[H^+]$, $[OH^-]$, $[NH_4^+]$, $[NH_3]$, and [P] may all be regarded to be constant with time. The rate equations can then be solved to give

$$[e_{aq}^-] = (1 + k_R[R]_i t)^{-1}\{U \exp(-k_u t) + V \exp(-k_v t)\} \quad (13)$$

where

$$k_u + k_v = k_q + k_p[P], \qquad k_u k_v = k_p[P]k_s$$

$$U + V = [e_{aq}^-]_i, \qquad k_v U + k_u V = ([e_{aq}^-]_i + [H]_i)k_s$$

$$k_q = k_5'[NH_4^+] + k_{-5}[NH_3] + k_1'[H^+] + k_{-1} + k_2 + k_{-2}[OH^-]$$

$$k_s = k_{-5}[NH_3] + k_{-1} + k_{-2}[OH^-]$$

From the definition, k_q is the equilibration rate, while k_s is a total rate of producing e_{aq}^- from H atom.

Analytic procedures similar to those described in the preceding subsection were used with some modifications. Parameter $k_R[R]_i$ was determined so that the data at 0.4 and 0.8 Gy/pulse should match after being multiplied by $(1 + k_R[R]_i t)/[R]_i$. An approximate zero-dose decay curve, $[e_{aq}^-](1 + k_R[R]_i t)$, was then analyzed as an overlap of two exponential decays. It is noted that k_v for the second step was at most 5% of k_u for the first step and that k_v/k_u tended to decrease with temperature.

Similarly to the analysis on $HClO_4$ solutions, all the data were then examined by a curve-fitting method that uses eq 13 and the above-obtained $k_R[R]_i$, U, k_u, V, and k_v as initial parameters. Though some uncertainty was inevitable, data at the two different pulse doses could be fitted satisfactorily with a consistent set of parameters, from which values of k_q, k_s, and $k_p[P]$ were calculated.

Among the data at 0.1 m in $[NH_4^+]$, those above 100 °C were analyzed only to evaluate K_5. For each datum $[e_{aq}^-]_i$ was estimated indirectly from pulse dose and $G_{e_{aq}^-}\epsilon(824)$, where $\epsilon(824)$ is an absorption coefficient of e_{aq}^- at 824 nm. A comment is added about the temperature dependence of $G_{e_{aq}^-}\epsilon_{max}$, where ϵ_{max} is the maximum absorption coefficient. It was found from the experiments on 5×10^{-3} m $[NH_4^+]$ solutions and on pure water that $G_{e_{aq}^-}\epsilon_{max}$ increases by about 1.2 times in going from 25 to 200 °C, in agreement with our previous results.[9] However, whereas the previous data suggested a monotonous increase up to 250 °C,[9] the present $G_{e_{aq}^-}\epsilon_{max}$ at 225 and at 250 °C were, respectively, 0.97 ± 0.03 and 0.93 ± 0.05 times that at 200 °C. The discrepancy may be due to error in dose monitoring in the earlier experiments with a different apparatus.

Equilibrium Constants. The equilibrium constant K_1 was evaluated from parameter B of the $HClO_4$ system by using the relationship

$$B^{-1} - 1 = [H]_{eq}/[e_{aq}^-]_{eq} = K_1[H^+]_0 \quad (14)$$

Examples for the plot of $[H]_{eq}/[e_{aq}^-]_{eq}$ against $[H^+]_0$ are shown in Figure 2. Though error ranges are large for the data below 175 °C, the proportionality of eq 14 is found at all temperatures. Likewise, K_5 was evaluated from the relation

$$k_q/k_s - 1 = [H]_{eq}/[e_{aq}^-]_{eq} = k_5'[NH_4^+]/(k_{-5}[NH_3]) = K_5\gamma^2[NH_4^+]/[NH_3] \quad (15)$$

Here, γ was substituted by a mean activity coefficient for NH_4^+ and OH^-, and it was calculated from an experimental formula by Hitch and Mesmer.[26] Examples of the plot for eq 15 are shown in Figure 3. It is seen that at each temperature the data at two different $[NH_4^+]$, 5×10^{-3} and 0.1 m, are consistent within uncertainty. Hence, the use of γ for NH_4^+ and OH^- may be considered not to introduce large error in K_5.

A van't Hoff plot of the obtained K_1 is shown in Figure 4, where values calculated from K_5, by using K_6 in ref 26 and K_W in ref 27, are also plotted. The two sets of K_1 agree fairly well, the discrepancy at temperatures above 175 °C being less than 15% (in the linear scale). It is noted that our previous tentative values of K_1 were reasonable above 200 °C[16,17] but that they were considerably underestimated at the lower temperatures. As seen, $\log K_1$ or $pK_a(H)$ reduces from 9.6 to about 6.2 upon temperature elevation from 25 to 250 °C. Also evident is concave upward curvature in a range corresponding to temperature above 100 °C. It indicates that $\Delta C_p°(1)$ is positive, or that dissociation of H atom is less favored at high temperatures than expected from linear extrapolation of the dependence below 100 °C, probably because of reduction in the dielectric constant of water. For comparison $-\log K_w$ is also plotted in Figure 4. The approximate parallelism of $\log K_1$ and $-\log K_w$ shows that $\Delta H°(1)$ is nearly

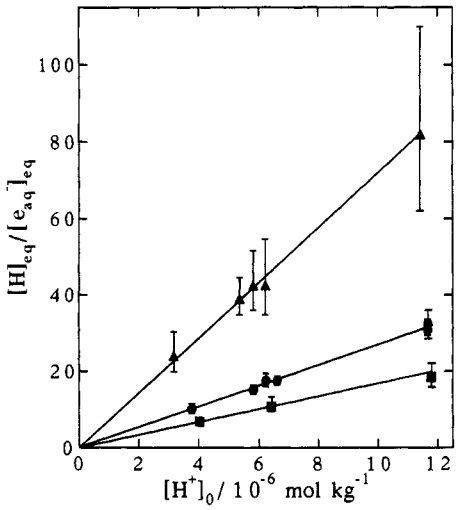

Figure 2. Dependence of equilibrium ratio of [H] to $[e_{aq}^-]$ in $HClO_4$ solutions upon $[H^+]_0$. ▲ 150 °C; ● 200 °C; ■ 250 °C. The slopes of the lines give K_1 at these temperatures. Each error bar represents uncertainty in the analysis and does not include possible systematic error.

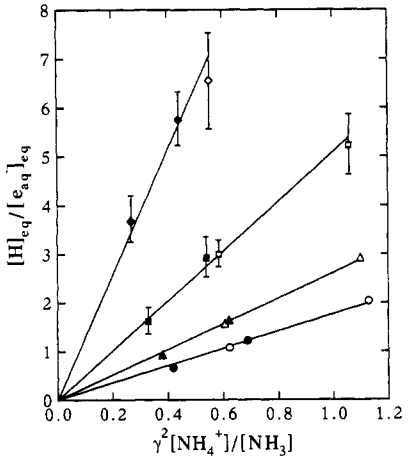

Figure 3. Dependence of equilibrium ratio of [H] to $[e_{aq}^-]$ on $\gamma^2[NH_4^+]/[NH_3]$. ○, ● 100 °C; △, ▲ 150 °C; □, ■ 200 °C; ◇, ◆ 250 °C. Open symbols represent data at 5×10^{-3} *m* in $[NH_4^+]$, and closed symbols do those at 0.1 *m* in $[NH_4^+]$. γ is a mean activity coefficient, and the slopes of the lines give K_5. The same comment as in Figure 2 applies to the error bars.

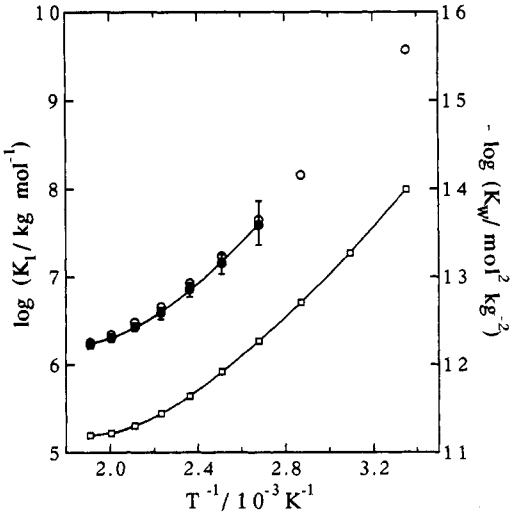

Figure 4. Temperature dependence of equilibrium constant K_1. ● data from $HClO_4$ solutions; ○ data calculated from K_5 in Figure 5. The error bars are for ●, and the same comment as in Figure 2 applies to them. The two sets of K_1 data agree fairly well. Also plotted are $-\log K_W$, □, from ref 27.

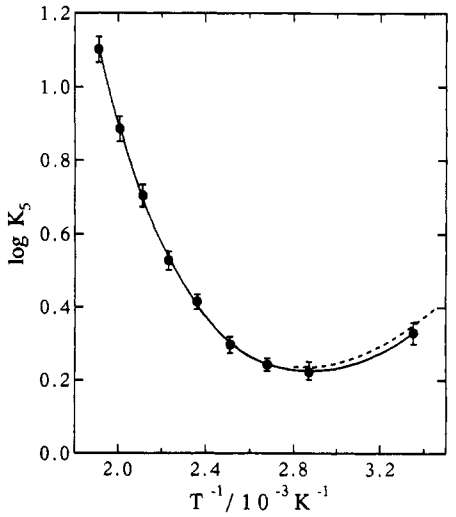

Figure 5. Temperature dependence of equilibrium constant K_5. ● present data from NH_4^+/NH_3 solutions; broken line from ref 17. The same comment as in Figure 2 applies to the error bars.

equal to $-\Delta H°(4)$ throughout the temperature range. The shift of the two curves, on the other hand, represents that the difference between $\Delta S°(1)$ and $-\Delta S°(4)$, which is due mainly to large $S°(e_{aq}^-)$ as discussed by Han and Bartels,[20] persists up to high temperatures.

Results on K_5 are displayed in Figure 5. The present K_5 at 25 and at 75 °C agree very well with the data by Schwarz.[17] The curvature of log K_5 shows that $\Delta H°(5)$, being a small negative value at 25 °C, changes its sign on account of positive $\Delta C_p°(5)$. Since both $\Delta C_p°(4)$ and $\Delta C_p°(6)$ are known to decrease rapidly above 100 °C, and comparable variation (in a reversed direction) is inferred for both $\Delta C_p°(1)$ and $\Delta C_p°(5)$, no direct thermodynamic analysis was undertaken either on K_1 or on K_5. As described below, K_2 was analyzed instead.

Cobble et al. have shown that when an identical number of charged species exist on both sides of an equilibrium, $\Delta C_p°$ is generally almost constant up to 300 °C as a result of approximate compensation of the changes in ionic $C_p°$.[30] Since equilibrium 2 is in such a form, K_1 and K_5 were converted into K_2 by using K_W from ref 27 or K_6 from ref 26. The results are shown in Figure 6. As is natural from the approximate parallelism of log K_1 and $-\log K_W$ in Figure 4, variation of K_2 is very small. It is noticed that the data at high temperatures are significantly above a curve predicted by Schwarz.[17] Analysis of K_2 was made by fitting to eq 16, where linear variation of $\Delta C_p°(2)$ was allowed for

$$\ln K_2 = -\Delta G°(2)/RT = -[\Delta H°_{25}(2) + \int \Delta C_p°(2)\,dT - T\{\Delta S°_{25}(2) + \int \Delta C_p°(2)/T\,dT\}]/RT \quad (16)$$

$$\Delta C_p°(2) = \Delta C_p°_{25}(2) + \alpha(T - 298.15)$$

Here R ane T are the gas constant and the absolute temperature, respectively. The suffix 25 denotes a thermodynamic quantity at 25 °C. Since there were only two points below 100 °C, the Schwarz' data[17] were included in the fitting analysis after conversion into K_2. On the other hand, the present K_2 data from $HClO_4$ solutions below 200 °C were excluded as being uncertain. A simple linearized least-squares method was applied with assigned uncertainties, which were ±0.04 below 75 °C, ±0.06 to ± 0.1 up to 200 °C, and ±0.12 above 200 °C. (The values are in ln K_2 and are supposed not to include systematic error. But, see below.) The result gave a solid curve drawn in Figure 6, and α was 0.017 ± 0.080 cal K^{-2} mol^{-1}, the small magnitude of which is in accord with the expectation of a nearly constant $\Delta C_p°(2)$.

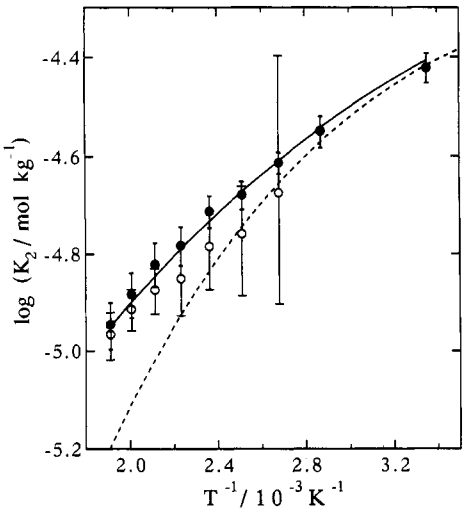

Figure 6. Temperature dependence of equilibrium constant K_2. ○ data based on K_1 from $HClO_4$ solutions; ● data based on K_5 from NH_4^+/NH_3 solutions. The solid curve represents the result of fitting to eq 16, and the broken one does a curve predicted in ref 17. The larger error bars are for ○ and the smaller ones for ●. The same comment as in Figure 2 applies to these error bars.

TABLE 1: Thermodynamic Changes Associated with Reactions 2, 1, and 5[a]

temp, °C	$\Delta G°$/kcal mol^{-1}	$\Delta H°$/kcal mol^{-1}	$\Delta S°$/cal K^{-1} mol^{-1}	$\Delta C_p°$/cal K^{-1} mol^{-1}
		reaction 2		
25	6.01 ± 0.04	−1.1 ± 0.2	−23.8 ± 0.8	−8.2 ± 6.4
250	11.85 ± 0.21	−2.5 ± 1.0	−27.4 ± 2.3	−4.4 ± 12.8
		reaction 1[b]		
25	−13.08 ± 0.04	−14.4 ± 0.2	−4.5 ± 0.8	43.6 ± 6.5
250	−14.95 ± 0.22	−1.8 ± 1.2	25.2 ± 2.7	118 ± 17
		reaction 5[c]		
25	−0.47 ± 0.04	−2.0 ± 0.3	−5.3 ± 0.8	43.9 ± 9.8
250	−2.62 ± 0.25	12.9 ± 1.4	29.6 ± 3.0	133 ± 28

[a] 1 cal mol^{-1} = 4.184 J mol^{-1}. [b] Calculated by using the data on reaction 4 in ref 27 except for $\Delta C_p°$ (4), which is from ref 33. [c] Calculated by using the data on reaction 6 in ref 26.

The obtained other thermodynamic quantities for reaction 2 at both 25 and 250 °C are listed in Table 1, where the standard state is taken to be hypothetical ideal solution at 1 m. Each error range was estimated as a sum of uncertainty predicted by the least-squares method plus that caused by possible systematic error in K_2. The latter was calculated under a supposition that systematic error in ln K_2 increases linearly with T from ±0.049 at 25 °C to ±0.13 at 250 °C. This assignment includes error due to uncertainty in $G_H/G_{e^-_{aq}}$ at high temperatures. It is added that pressure dependence of the thermodynamic quantity, which is usually very small in the pressure range of the present experiments, is ignored.

The listed 25 °C values naturally agree well with those by Schwarz except $\Delta C_p°_{25}(2)$, for which he gave a rough estimate of −15 ± 10 cal K^{-1} mol^{-1} based on direct analysis of K_5.[17] Admitting that the present analysis relies on the accuracy of K_6 by Hitch and Mesmer,[26] we presume that −8.2 ± 6.4 cal K^{-1} mol^{-1} is a better estimate. Thermodynamic quantities for equilibria 1 and 5, derived from those on equilibria 2, 4, and 6 are also listed in Table 1. Unlike the case of equilibrium 2, every property except for $\Delta G°$ depends strongly on temperature, but the magnitude of variation in each property is very similar with these two equilibria. In fact, $\Delta C_p°(1)$ and $\Delta C_p°(5)$ are both fairly large and temperature dependent, but they are nearly equal up to 250 °C. It is added that upon extrapolation $\Delta H°(1)$ is estimated to be zero at about 270 °C.

TABLE 2: Thermodynamic Changes Associated with Hydration Reactions

temp °C	$\Delta G°$/kcal mol^{-1}	$\Delta H°$/kcal mol^{-1}	$\Delta S°$/cal K^{-1} mol^{-1}
	$H^+_{gas} + e^-_{gas} \rightarrow H^+_{aq} + e^-_{aq}$[a]		
25	−296.7 ± 0.6	−301.6 ± 0.9	−16.6 ± 1.9
250	−291.7 ± 1.3	−309.3 ± 2.5	−33.6 ± 5.2
	$H^+_{gas} + OH^-_{gas} \rightarrow H^+_{aq} + OH^-_{aq}$[b]		
25	−367.0 ± 0.9	−387.8 ± 0.9	−69.8 ± 0.2
250	−348.3 ± 1.0	−400.4 ± 1.1	−99.5 ± 1.3

[a] Calculated by using the data on H^+_{gas} and e^-_{gas} in ref 38. [b] Calculated by using the data on OH^-_{gas} and H_2O_{liq} in ref 38 in combination with those on reaction 4 in ref 27.

Thermodynamics of e^-_{aq}. The results on equilibrium 1 can be combined with the data on aqueous H atom to estimate the thermodynamic properties of e^-_{aq}. Roduner and Bartels concluded in a recent study that the thermodynamics of hydration of the H atom are best approximated by those of H_2 having a similar polarizability.[31] Then, $\Delta G°_f(H_{aq})$, $\Delta H°_f(H_{aq})$, and $S°(H_{aq})$ at 25 °C are evaluated respectively to be 52.8 ± 0.5, 51.1 ± 0.8 kcal mol^{-1}, and 9.9 ± 1.5 cal K^{-1} mol^{-1} by using the data for hydration of H_2.[32] The uncertainties are assigned by taking into account of the corresponding data for hydration of He and Ne.[32] (The convention employed here is that irrespective of temperature $\Delta G°_f = \Delta H°_f = S° = C_p° = 0$ for H^+_{aq} and that the standard state for gaseous species is ideal gas at 0.1 MPa. A top bar for representing a partial molar quantity is omitted.) It follows that $\Delta G°_f(e^-_{aq})$, $\Delta H°_f(e^-_{aq})$, and $S°(e^-_{aq})$ at 25 °C are 65.9 ± 0.5, 65.6 ± 0.9 kcal mol^{-1}, and 14.5 ± 1.9 cal K^{-1} mol^{-1}, respectively. The values differ slightly from those by Schwarz who used different data for H_{aq} estimated on the basis of He analogy for the hydration energetics.[17]

Discussion is first made about $C_p°(e^-_{aq})$ at 25 °C. Since $C_p°(H_{aq})$ at 25 °C may be evaluated to be 39 ± 9 cal K^{-1} mol^{-1} by using $\Delta C_p°$ for hydration of H_2, 34 cal K^{-1} mol^{-1},[32] $C_p°(e^-_{aq})$ at 25 °C then becomes −4 ± 11 cal K^{-1} mol^{-1}, which is significantly larger than $C_p°$ of classical anions. Though OH^- is rather special, $C_p°(OH^-_{aq})$ is reported to be −34 cal K^{-1} mol^{-1},[33] and $C_p°(I^-_{aq})$ is −29 cal K^{-1} mol^{-1}.[34] Note that in the present convention $C_p°$ of an aqueous anion includes heat capacity associated with H^+_{aq}, and that the comparison is limited to within anions. The comparatively large $C_p°(e^-_{aq})$ indicates that there are a larger number of thermally excitable modes in the vicinity of e^-_{aq}. The presence of these modes may be attributed to loose and fluctuating solvation structure of e^-_{aq} suggested by molecular dynamics calculations,[35,36] and naturally the feature of $C_p°(e^-_{aq})$ may be taken to be associated with the large magnitude of $S°(e^-_{aq})$, which was emphasized by Han and Bartels as showing the structure-breaking property of e^-_{aq}.[20]

Though it may be an acknowledged fact, weaker solvation of e^-_{aq} as compared to classical anions is evident from $\Delta H°$ for hydration reaction from gas phase. As can be estimated from the data in Table 2, $\Delta H°_{hyd}(e^-) - \Delta H°_{hyd}(OH^-)$ amounts to 86 kcal mol^{-1}, and in another comparison $\Delta H°_{hyd}(e^-) - \Delta H°_{hyd}(I^-)$ is 32.7 kcal mol^{-1}.[37,38] It has been known that the Born theory,[39] being combined with appropriate assignment of ionic radii, accounts very well for the energetics of ionic hydration. In this theory $\Delta G°_{hyd}$ and $\Delta H°_{hyd}$ for a single ion with charge Ze are given, respectively, as

$$\Delta G°_{hyd} = -(8\pi\epsilon_0 r)^{-1}(Ze)^2 N_A(1 - \epsilon_s^{-1}) \quad (17a)$$

$$\Delta H°_{hyd} = \Delta G°_{hyd} + (8\pi\epsilon_0 r)^{-1}\epsilon_s^{-2}(Ze)^2 N_A T(\partial\epsilon_s/\partial T)_p \quad (17b)$$

where r, ϵ_0, ϵ_s, and N_A denote, respectively, radius, the dielectric constant of vacuum, the relative static dielectric constant of water, and the Avogadro number. The applicability of eq 17b was

recently confirmed for many classical ions, including even OH^-, by adopting a new method for assigning r.[40] It has also been found that the rather surprising applicability of the primitive theory results from the compensation of the dielectric saturation effect by the electrostriction effect within the inner shells.[41] However, the above differences in $\Delta H°_{hyd}$ are evidently difficult to be explained by the radius of e^-_{aq}. They may reflect that part of the electron cloud resides outside the cavity, but anyway can be taken to represent considerably different inner-shell interactions.

To discuss thermodynamic properties at high temperature, a simple analysis was made on the reported H_2 solubility data,[42] which led to an estimate that at 250 °C $\Delta G°_f(H_{aq}) = 52.0 \pm 1.1$ kcal mol^{-1}, $\Delta H°_f(H_{aq}) = 57.6 \pm 2.0$ kcal mol^{-1}, and $S°(H_{aq}) = 28.1 \pm 4.0$ cal K^{-1} mol^{-1}. The uncertainties were again assigned on the basis of similar analyses on the high temperature solubility of He and Ne.[43] These values may be used to derive formation data for e^-_{aq} at 250 °C, but for convenience we list in Table 2 $\Delta G°$, $\Delta H°$, and $\Delta S°$ for $H^+_{gas} + e^-_{gas} \rightarrow H^+_{aq} + e^-_{aq}$ together with those for $H^+_{gas} + OH^-_{gas} \rightarrow H^+_{aq} + OH^-_{aq}$.

One can first see that in the both cases $\Delta G°_{hyd}$ increases but $\Delta H°_{hyd}$ decreases on going from 25 to 250 °C. These trends are qualitatively as expected from eq 17 and the temperature dependence of ϵ_s which reduces from 78 at 25 °C to 27 at 250 °C.[44] It is known that below 100 °C $\Delta C_p°_{hyd}$ of ionic species, corresponding to the temperature coefficient for $\Delta H°_{hyd}$, is hardly accounted for by an expression obtained by differentiation of eq 17b. However, as Cobble et al. have shown for examples of $\Delta C_p°_{hyd}(Na^+,Cl^-)$ and others,[45] the temperature dependence above 150 °C, where $\Delta C_p°_{hyd}$ falls rapidly with temperature, rather conforms to the simple expression derived from the Born theory. Quantitative agreement may not be expected in general with regard to $\Delta C_p°_{hyd}$, but it is natural that interactions involving remote solvation shells become more important with reduction in ϵ_s, so that the trend predicted by the Born theory should tend to dominate at high temperatures.

As seen in Table 2, the decrease in $\Delta H°_{hyd}(H^+,e^-)$ is smaller by 4.9 kcal mol^{-1} than that in $\Delta H°_{hyd}(H^+,OH^-)$. This difference compares roughly with a value 7.2 kcal mol^{-1} calculated by assuming that the difference between $C_p°(e^-_{aq})$ and $C_p°(OH^-_{aq})$ at 25 °C is maintained up to 250 °C.[46] Although the limited solubility data for H_2 do not allow accurate estimation of $C_p°(H_{aq})$ or $C_p°(e^-_{aq})$ at high temperatures, $C_p°(e^-_{aq})$ is presumed to vary roughly in parallel with $C_p°(OH^-_{aq})$, which decreases to about −101 cal K^{-1} mol^{-1} at 250 °C. A molecular dynamics calculation on e^-_{aq} by Wallqvist et al. indicated a temperature effect which may be viewed to be corresponding to the present results.[36] According to their calculation, an average number of water molecules in the first shell decreases from 6 to 5 upon temperature elevation from 300 to 373 K, but simultaneously the total energy of the system, related to $\Delta H°_{hyd}$, decreases primarily due to reduction in the interaction energy between the excess electron and water molecules in outer solvation shells.

Implicit in the above discussion is a view that e^-_{aq} is stabilized in a cavitylike region surrounded by water molecules. No detailed argument is given here in relation to a solvent–anion complex model by Tuttle and Golden[47] or to a $(OH^-\cdots H_3O)$ model by Robinson et al.,[48] but the thermodynamic data do not appear to favor these models.

Rate Constants. The rate constant k_1 was obtained from k_{eq} for $HClO_4$ solutions. It can readily be derived that

$$k_{eq}K_1[H^+]_0/(1 + K_1[H^+]_0) = k_1[H^+]_0 + k_2 \quad (18)$$

Examples of the plot for eq 18 are shown in Figure 7, where one first confirms that reaction 1 is primarily responsible for the equilibration in the present $HClO_4$ solutions. It was possible to evaluate k_1 from the slopes reliably up to 250 °C, the uncertainty

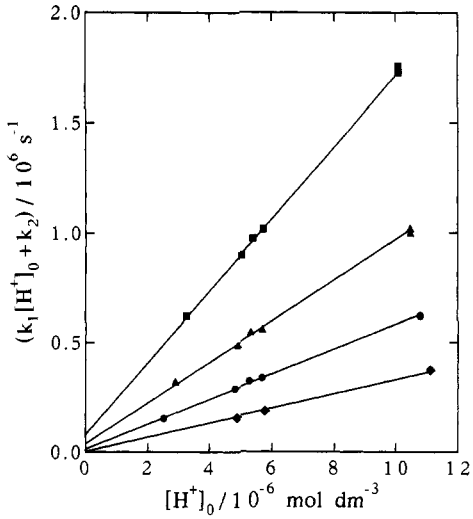

Figure 7. Plots of $k_1[H^+]_0 + k_2$ against $[H^+]_0$. ● 50 °C; ● 100 °C; ▲ 150 °C; ■ 200 °C. The data were calculated from K_1 and equilibration rates in $HClO_4$ solutions. Uncertainty in each datum, including systematic error, is less than ±9% up to 200 °C.

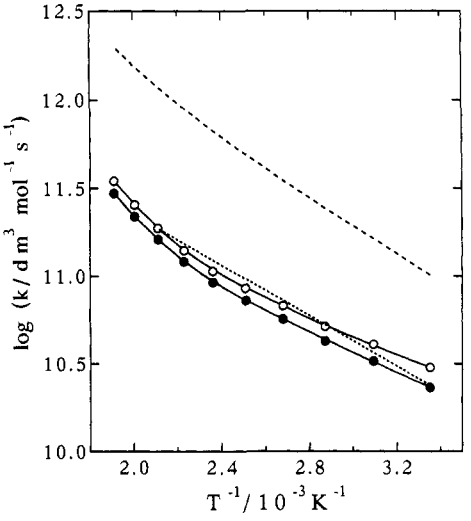

Figure 8. Arrhenius plot of rate constant k_1 (●), showing concave upward curvature at high temperatures. Calculated k_D (broken line) and k_{react} (○) for reaction 1 are also shown. The dotted line represents k_1 data from ref 19.

being estimated to be less than ±12% including systematic error. As for the intercepts, large uncertainty allowed merely to confirm that they agree roughly with values given by extrapolation of recent Schwarz' k_2 data showing an activation energy of 7.5 kcal mol^{-1}.[21] It was also found that the results on the ethanol solution, where the zero-dose decay rate of e^-_{aq} should be $k_1[H^+]_0 + k_2$, are consistent with those in Figure 7.

The Arrhenius plot of k_1, shown in Figure 8, is almost linear between 25 and 100 °C, where an activation energy is 2.6 kcal mol^{-1}. This value is in good agreement with relatively recent data by others,[25] though significantly larger values have also been reported.[25] In a region corresponding to temperature above 150 °C the plot of k_1 is clearly curved concave upward, suggesting that the reaction is accelerated with reduction in the dielectric constant ϵ_s. Unlike our results hardly any curvature is seen in the k_1 data by Elliot et al.[19] though the discrepancy between the two sets of k_1 is not very large in the common temperature range below 200 °C. (Their data indicate an activation energy of about 3.3 kcal mol^{-1}.) It is noted that the curvature of k_1 is not so small as to vanish in a plot in the molal unit.

As has been remarked by others,[49] k_1 is not truly diffusion-controlled. To analyze the temperature dependence of k_1, reaction

1 is modeled as follows:[50,51]

$$e^-_{aq} + H_3O^+ \underset{k_{-D}}{\overset{k_D}{\rightleftharpoons}} e^-_{aq}\cdots H_3O^+ \underset{k_{-11}}{\overset{k_{11}}{\rightleftharpoons}} H\cdots H_2O \underset{k_{-12}}{\overset{k_{12}}{\rightleftharpoons}} H + H_2O \qquad (19)$$

where $e^-_{aq}\cdots H_3O^+$ and $H\cdots H_2O$ represent close-contact encounter complexes, and each k denotes a rate constant for the respective step. The reaction is supposed to proceed via a transition state in the step from from $e^-_{aq}\cdots H_3O^+$ to $H\cdots H_2O$. Han and Bartels argued that reaction 1 should be viewed as an H^+ transfer reaction rather than as an electron-transfer reaction.[52] The three-step mechanism itself is a general one. When $k_{12} \gg k_{-11}$ and a steady state is assumed for the both encounter complexes, $1/k_1$ is expressed as[50,51]

$$1/k_1 = 1/k_D + 1/k_{react} \qquad (20)$$

$$k_{react} = K_{A1}k_{11}$$

where K_{A1} is k_D/k_{-D}, i.e., a formation constant of $e^-_{aq}\cdots H_3O^+$ expressed in the molar unit. The diffusion-controlled rate constant k_D is given by the Smoluchowski–Debye equation, which is written for the present purpose as[53]

$$k_D = 4\pi f r_{ec}(D_{H^+} + D_{e^-_{aq}})N_A \qquad (21a)$$

$$f = W_r/[\{\exp(W_r/RT) - 1\}RT] \qquad (21b)$$

$$W_r = -e^2N_A/(4\pi\epsilon_0\epsilon_s r_{ec}) \qquad (21c)$$

Here r_{ec}, D_{H^+}, and $D_{e^-_{aq}}$ express, respectively, distance between e^-_{aq} and H_3O^+ in the encounter complex, the diffusion coefficient of H^+, and that of e^-_{aq}. W_r corresponds to electrostatic work for bringing the two species to r_{ec}, and f is called the Debye factor. In the evaluation D_{H^+} was calculated from the literature data for the limiting equivalent conductance of H^+.[54] Since no high-temperature data were available for $D_{e^-_{aq}}$, an activation energy of 4.8 kcal mol^{-1}, recently confirmed by Schmidt et al,[55] was used to estimate $D_{e^-_{aq}}$ above 100 °C. $D_{e^-_{aq}}$ at 250 °C is then 1.6×10^{-3} cm^2 s^{-1}, which far exceeds D_{OH^-} of 3.6×10^{-4} cm^2 s^{-1} or D_{H^+} of 4.1×10^{-4} cm^2 s^{-1} at 250 °C.[54] A constant r_{ec} of 0.5 nm was assumed, and f then increases from 1.9 at 25 °C to 2.6 at 250 °C. Though r_{ec} is not a sensitive parameter with regard to k_D for oppositely charged species, it is to influence K_{A1} as described below.

The calculated k_D and k_{react} are drawn in Figure 8. It is found that k_D, being 4.4 to 7.4 times k_1 at the same temperature, does not much affect the temperature dependence of k_1, and that k_{react} is mainly responsible for the curvature of k_1. To advance analysis, K_{A1} is approximated as[56]

$$K_{A1} = 4\pi r_{ec}^2\, \delta r N_A \exp(-W_r/RT) \qquad (22)$$

Here δr denotes width of possible r_{ec} and is taken to be 0.1 nm. The picture here is essentially the same as that for ionic reaction by Brønsted, Christiansen, and Scatchard.[57] Since for r_{ec} of 0.5 nm, W_r changes from −0.85 kcal mol^{-1} at 25 °C to −2.5 kcal mol^{-1} at 250 °C, K_{A1} thereby increases by 2.6 times. As seen from the plots of K_{A1} and k_{11} in Figure 9, the curvature of k_{react} may be attributed largely to K_{A1} or its dependence on ϵ_s. It was noticed that an assumption of 0.35 nm for r_{ec} would lead to a linear Arrhenius plot for k_{11}. Naturally, real interionic potential must be different from W_r of eq 21c which is based on a simple theory of dielectric continuum. Yet, the analysis indicates that the presence of an acceleration effect other than that from the Debye factor is quite probable. It is added that the effect of dielectric constant has also been demonstrated with several e^-_{solv} reactions

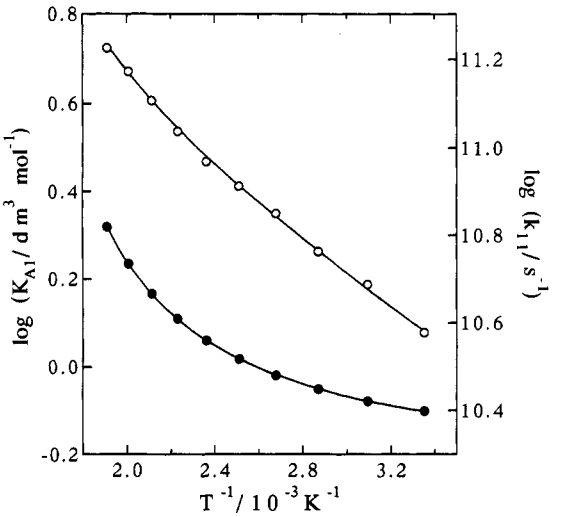

Figure 9. Temperature dependence of equilibrium constant K_{A1} (●) and that of rate constant k_{11} (○). These illustrate possible sources of the nonlinearity in the Arrhenius plot of k_1 in Figure 8.

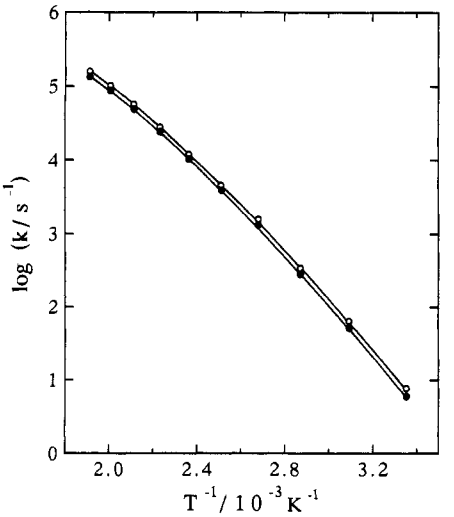

Figure 10. Arrhenius plot of rate constant k_{-1} (●), showing concave downward curvature. Temperature dependence of $K_{A1}'k_{-11}$ (○) is also illustrated.

by varying composition of alcohol–water mixture at room temperature.[58,59]

Elliot et al have already analyzed the temperature dependence of k_1 by using eq 20.[19] However, k_{react} was not factorized, since they regarded their Arrhenius plot of k_{react} to be linear below 200 °C. It is noted that the discrepancy is not ascribable to their use of D_{OH^-} as a substitute for $D_{e^-_{aq}}$ in calculating k_D. As described later, the present picture on the acceleration of k_{react} applies also to the result on k_5.

The rate constant k_{-1} was obtained as k_1/K_1. Uncertainty in k_{-1} increased with temperature: ±13, ±16, ±22, and ±35%, respectively, at 25, 100, 200, and 250 °C, including systematic error. Though displaying an Arrhenius plot of k_{-1} may seem redundant, it is shown in Figure 10 to illustrate its concave downward curvature. An activation energy below 100 °C is about 16 kcal mol^{-1}, but slight curvature, which accounts for most of the change in $\Delta H(1)$, is seen to be present even in this region.[60] In the present model, k_{-1} is given as

$$k_{-1} = \{k_{-D}/(k_{-D} + k_{11})\}K_{A1}'k_{-11} \qquad (23)$$

where K_{A1}' is k_{-12}/k_{12}. Since k_{-D} is calculated to be 3.4–6.4 times k_{11}, and $k_{-D}/(k_{-D} + k_{11})$ changes little with temperature, the curvature of the plot of k_{-1} has to be ascribed to $K_{A1}'k_{-11}$, which is drawn also in Figure 10. This aspect is like that in the

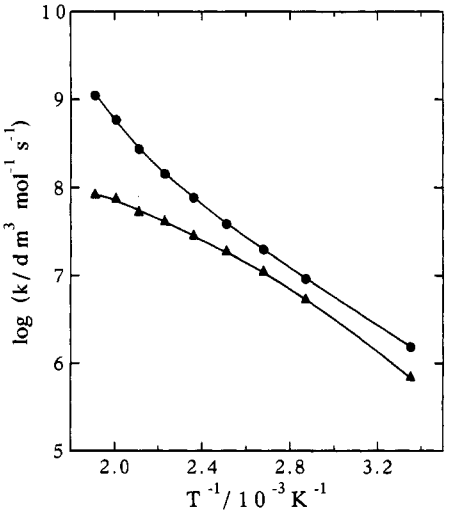

Figure 11. Arrhenius plots of rate constants k_5 (●) and k_{-5} (▲), showing mutually opposite curvatures. k_5 is corrected for the effect of ionic strength by use of γ^2 for NH_4^+ and OH^-.

case of k_1. However, here the responsible factor is most probably k_{-11} rather than K_{A1}', and log k_{-11} is presumed to curve similarly to log $K_{A1}'k_{-11}$. In the present model k_{-11} is expressed as

$$k_{-11} = k_{11} \exp(-\Delta G^\circ_{ec}/RT) \qquad (24)$$

where ΔG°_{ec} denotes $\Delta G^\circ_f(e_{aq}^-\cdots H_3O^+) - \Delta G^\circ_f(H\cdots H_2O)$. The presumed concave downward curvature of log k_{-11} is likely to be attributed to an effect from ΔG°_{ec}. Since the activation free energy for k_{11} is apparently much smaller than that of k_{-11}, it seems natural that the latter depends more strongly on ΔG°_{ec} than the former, as inferred, for example, from the well-known Marcus equation relating a free energy of activation to ΔG° of the reaction.[51] The nonlinearity in log k_{-11} is then deemed to be caused by the difference between $C_p^\circ(H\cdots H_2O)$ and $C_p^\circ(e_{aq}^-\cdots H_3O^+)$, for which the decrease in ϵ_s must be partly responsible.

In the evaluation of k_5 and k_{-5} it was necessary first to correct the equilibration rate k_q for the effects of reactions 1 and 2. For this purpose k_{-2} above 100 °C was estimated by extrapolating k_{-2} data by Han and Bartels[20] with an assumption that the Arrhenius plot is linear in the molar unit, and k_2 was calculated as $k_{-2}K_2$. A ratio $(k_1'[H^+] + k_{-1} + k_2 + k_{-2}[OH^-])/k_q$ increased with temperature, but owing to lowering of pH, $(k_2 + k_{-2}[OH^-])/k_q$ was relatively small at high temperatures, where k_2 and k_{-2} were uncertain. To note the degree of correction at 250 °C, $(k_1'[H^+] + k_{-1})/k_q$ and $(k_2 + k_{-2}[OH^-])/k_q$ were, respectively, 0.23 and 0.04 for a solution 5×10^{-3} *m* in $[NH_4^+]$ and 6.7×10^{-3} *m* in $[NH_3]$.

k_5' and k_{-5} were then calculated by using $[H]_{eq}/[e_{aq}^-]_{eq}$, and k_5' was divided by γ^2 to obtain k_5. Uncertainty in k_5 was less than ±28%, while that in k_{-5} increased with temperature from ±20% at 25 °C to ±32% at 250 °C. In the both cases about half was due to possible systematic errors that are presumed to vary only slowly with temperature. Arrhenius plots of k_5 and k_{-5} are shown in Figure 11. The two rate constants are of similar magnitude in correspondence to the small $\Delta G^\circ(5)$. An approximate activation energy calculated from the data at 25 and 75 °C is 7.4 and 8.4 kcal mol^{-1}, respectively, for k_5 and k_{-5}, but neither log k_5 nor log k_{-5} may be strictly linear in that range. (The former value agrees well with 7.2 kcal mol^{-1} obtained by Schwarz at an ionic strength of 0.05 *m*.[17]) In a region corresponding to temperature above 150 °C these plots are clearly curved in mutually opposite directions.

The curvatures of k_5 and k_{-5} may be discussed with a model analogous to the one in eq 19. Since k_5 is apparently much smaller than the diffusion-controlled limit, k_5 may be equated with k_{react} or $K_{A5}k_{51}$, where K_{A5} and k_{51} are, respectively, a formation constant for $e_{aq}^-\cdots NH_4^+$ and a rate constant for the step from $e_{aq}^-\cdots NH_4^+$ to $H\cdots NH_3$. It was found that deviation from linearity in log k_5 is somewhat larger than that in log $K_{A1}k_{11}$ in Figure 8; the difference was such that r_{ec} in W_r would have to be assumed as 0.3 nm, instead of 0.35 nm, to make an Arrhenius plot of k_{51} linear. This may imply that the nonlinearity in log k_{51} is larger than in log k_{11}. The difference is, however, not very large, and an effect from K_{A5} must certainly be important here as well. On the other hand, a simple comparison between log $K_{A1}'k_{-11}$ in Figure 10 and log k_{-5}, disregarding the difference in the unit for the rate constant, showed that deviation from linearity is very similar. The results on the rate constants thus indicated substantial similarity in each of the two types of curvature.

Other researchers have also reported nonlinear Arrhenius plots in the studies of water radiolysis at high temperature. Christensen and Sehested have found that $k(e_{aq}^- + e_{aq}^-)$ possesses a maximum at 150 °C.[61] Such peculiar temperature dependence has also been observed on other reactions of e_{aq}^-.[19] Elliot, Buxton, and their co-workers have reported that a different kind of nonlinearity is quite often seen in the Arrhenius plots of those reactions whose rate constants at 25 °C are close to the diffusion-controlled limit.[7,19] Concave downward curvature was explained as representing a change from diffusion control at low temperature to reaction control at high temperature. The nonlinearities observed in the present study are of different kind, and they may possibly be significant in general with those reactions where a pair of ions are involved either as reactants or as products.

Some other comments are worthwhile. Influence of the equilibrium between e_{aq}^- and H_{aq} may have been overlooked in some past studies including those on the radiolysis of reactor cooling water. Strange pH dependence of $k(e_{aq}^- + e_{aq}^-)$ at high temperature, reported in the above-cited study,[61] may possibly be interpreted on the basis of this equilibrium. It is noted additionally that though Hartig and Getoff reported $k(H + H_2O \rightarrow H_2 + OH)$ to be about 550 s^{-1} at 25 °C,[63] estimation of the equilibrium constant, being combined with $k(H_2 + OH)$, indicates that it should be smaller than k_{-1}.[64]

Conclusion

The two series of measurements gave consistent results on the equilibrium between e_{aq}^- and H above 100 °C, and the data on the NH_4^+/NH_3 system below 100 °C agreed with those by Schwarz.[17] pK_a(H) was found to fall from 9.59 ± 0.03 at 25 °C to 6.24 ± 0.09 at 250 °C. Since pK_a(H) is presumed to be minimal at about 270 °C, the value at 280 °C, the temperature of a boiling water reactor, must be close to 6.2.

Thermodynamic analysis on equilibrium 2, which was made including data from the Schwarz' study,[17] led to an estimate for $C_p^\circ(e_{aq}^-)$ to be −4 ± 11 cal K^{-1} mol^{-1} at 25 °C. The probable value is larger than $C_p^\circ(I_{aq}^-)$ at 25 °C by about 25 cal K^{-1} mol^{-1}, reflecting the presence of a larger number of thermally excitable modes in the vicinity of e_{aq}^-. The relatively small temperature dependence of $\Delta H^\circ_{hyd}(H^+,e^-)$ was interpreted to arise from this extra contribution to $C_p^\circ(e_{aq}^-)$, which compensates for a remote-shell effect to reduce $C_p^\circ(e_{aq}^-)$ with temperature. The presumed inner-shell effect on $C_p^\circ(e_{aq}^-)$ implies that there may be gradual change in the structure of e_{aq}^- with temperature.

The Arrhenius plot of k_1 and that of k_5 both showed significant concave upward curvature in a region corresponding to temperature above 150 °C. Though reaction 1 is partially diffusion controlled, the analysis indicated that deviation from linearity in log k_{react} is similar in the two cases, and that substantial part of the effect must arise from reduction in ϵ_s tending to promote ionic association. The Arrhenius plot of k_{-1} and that of k_{-5} showed an opposite trend of concave downward curvature in the same region.

In pure water, reaction 1 must be the more important path for the equilibration between e^-_{aq} and H at high temperature, since $k_1[H^+]_0 + k_{-1}$ amounts to 7.3×10^5 s^{-1} at 250 °C, while $k_2 + k_{-2}[OH^-]_0$ is estimated to be about 2.3×10^5 s^{-1} at the same temperature.[62] To add presumed values for k_1 and k_{-1} at 280 °C, extrapolation of the Arrhenius plots with allowance for the curvatures leads, respectively, to 4.9×10^{11} dm^3 mol^{-1} s^{-1} and 2.2×10^5 s^{-1}.

Acknowledgment. The authors express thanks to Prof. Y. Katsumura and Dr. G. V. Buxton for valuable advice. Thanks are also due to Mr. T. Kawanishi for his help in operating the accelerator, to Dr. E. Tachikawa and Dr. S. Ohno for their support, and to the reviewers for their comments.

References and Notes

(1) Burns, W. G.; Moore, P. B. *Radiat. Eff.* **1976**, *30*, 233.
(2) Christensen, H. *Radiat. Phys. Chem.* **1980**, *18*, 147.
(3) Related recent papers are found in: *Water Chemistry of Nuclear Reactor Systems 5*; British Nuclear Energy Society, London, 1989; Vols. 1 and 2. *Proc. 1991 JAIF Int. Conf. Water Chemistry of Nuclear Power Plants*; Japan Atomic Industrial Forum, Tokyo, 1991.
(4) Sehested, K.; Christensen, H. *Radiat. Phys. Chem.* **1990**, *36*, 499. Christensen, H.; Sehested, K. *J. Phys. Chem.* **1988**, *92*, 3007, and earlier papers of the same authors.
(5) Buxton, G. V.; Wood, N. D.; Dyster, S. *J. Chem. Soc., Faraday Trans. 1* **1988**, *84*, 1113.
(6) Elliot, A. J. *Radiat. Phys. Chem.* **1989**, *34*, 753.
(7) Buxton, G. V.; Elliot, A. J. *J. Chem. Soc., Faraday Trans.* **1993**, *89*, 485.
(8) Pikaev, A. K.; Kabakchi, S. A.; Egorov, G. F. *Radiat. Phys. Chem.* **1988**, *31*, 789.
(9) Shiraishi, H.; Katsumura, Y.; Hiroishi, D.; Ishigure, K.; Washio, M. *J. Phys. Chem.* **1988**, *92*, 3011.
(10) Buxton, G. V.; Wood, N. D. *Radiat. Phys. Chem.* **1989**, *34*, 699.
(11) Katsumura, Y.; Yamamoto, S.; Hiroshi, D.; Ishigure, K. *Radiat. Phys. Chem.* **1992**, *39*, 383.
(12) Elliot, A. J.; Chenier, M. P.; Ouellette, D. C. *J. Chem. Soc., Faraday Trans.* **1993**, *89*, 1193.
(13) Hart, E. J.; Gordon, S.; Fielden, E. M. *J. Phys. Chem.* **1966**, *70*, 150.
(14) Fielden, E. M.; Hart, E. J. *Trans. Faraday Soc.* **1967**, *63*, 2975; **1968**, *64*, 3158.
(15) Hickel, B.; Sehested, K. *J. Phys. Chem.* **1985**, *89*, 5271.
(16) Shiraishi, H.; Sunaryo, G. R.; Ishigure, K. *Symp. Solvated Electron 25 Years After*; Argonne IL, 1990; Abst p 39.
(17) Schwarz, H. A. *J. Phys. Chem.* **1991**, *95*, 6697.
(18) The thermodynamic data for e^-_{aq} in ref 15 almost agree with the new values by Schwarz, but the agreement seems fortuitous in view of the later measurement on k_{-2} in ref 20 and that on k_2 in ref 21.
(19) Elliot, A. J.; McCracken, D. R.; Buxton, G. V.; Wood, N. D. *J. Chem. Soc., Faraday Trans.* **1990**, *86*, 1539.
(20) Han, P.; Bartels, D. M. *J. Phys. Chem.* **1990**, *94*, 7294; **1991**, *95*, 5367.
(21) Schwarz, H. A. *J. Phys. Chem.* **1992**, *96*, 8937.
(22) LaVerne, J. A.; Pimblott, S. M. *J. Phys. Chem.* **1993**, *97*, 3291.
(23) Michael, B. D.; Hart, E. J.; Schmidt, K. H. *J. Phys. Chem.* **1971**, *75*, 2798.
(24) Christensen, H.; Sehested, K. *J. Phys. Chem.* **1986**, *90*, 186.
(25) Buxton, G. V.; Greenstock, C. L.; Helman, W. P.; Ross, A. B. *J. Phys. Chem. Ref. Data* **1988**, *17*, 513.
(26) Hitch, B. F.; Mesmer, R. E. *J. Solution Chem.* **1976**, *5*, 667.
(27) Sweeton, F. H.; Mesmer, R. E.; Baes, Jr., C. F. *J. Solution Chem.* **1974**, *3*, 191.
(28) Katsumura, Y. Private communication.
(29) Integration of the kinetic equations is possible without approximation, if some of the rate constants for recombination reactions are assumed. Comparison between curves so calculated and those based on eq 11 suggested that error in the present analysis is probably within the uncertainty.
(30) Cobble, J. W.; Murray, Jr., R. C.; Turner, P. J.; Chen, K. *High-Temperature Thermodynamic Data for Species in Aqueous Solution*; NP-2400, San Diego CA, 1982; section 4.
(31) Roduner, E.; Bartels, D. M. *Ber. Bunsen-Ges. Phys. Chem.* **1992**, *96*, 1037.
(32) Wilhelm, E.; Battino, R.; Wilcock, R. J. *Chem. Rev.* **1977**, *77*, 219.
(33) Allred, G. C.; Woolley, E. M. *J. Chem. Thermodyn.* **1981**, *13*, 147.
(34) Desnoyers, J. E.; de Visser, C.; Perron, G.; Picker, P. *J. Solution Chem.* **1976**, *5*, 605.
(35) Rossky, P. J.; Schnitker, J. *J. Phys. Chem.* **1988**, *92*, 4277.
(36) Wallqvist, A.; Martyna, G.; Berne, B. J. *J. Phys. Chem.* **1988**, *92*, 1721.
(37) Based on $\Delta H°_f(I^-_{gas})$ from ref 38 and on $\Delta H°_f(I^-_{aq})$ from the CODATA recommended values: *J. Chem. Thermodyn.* **1978**, *10*, 903.
(38) *JANAF Thermochemical Tables*, 3rd ed.; Chase, Jr., M. W., Davies, C. A., Downey, Jr., J. R., Frurip, D. J., McDonald, R. A., Syverud, A. N. *J. Phys. Chem. Ref. Data* **1985**, *14*, Suppl. 1.
(39) Born, M. *Z. Phys.* **1920**, *1*, 45.
(40) Rashin, A. A.; Honig, B. *J. Phys. Chem.* **1985**, *89*, 5588.
(41) Jayaram, B.; Fine, R.; Sharp, K.; Honig, B. *J. Phys. Chem.* **1989**, *93*, 4320.
(42) Himmelblau, D. M. *J. Chem. Eng. Data* **1960**, *5*, 10.
(43) Potter II, R. W.; Clynne, M. A. *J. Solution Chem.* **1978**, *7*, 837.
(44) Akerlof, G. C.; Oshry, H. J. *J. Am. Chem. Soc.* **1950**, *72*, 2844.
(45) Cobble, J. W.; Murray, Jr., R. C. *Nature* **1981**, *291*, 566.
(46) The calculated value includes an effect from the fact that $C_p°(e^-_{gas})$ is smaller than $C_p°(OH^-_{gas})$ by 2.0 cal K^{-1} mol^{-1}.
(47) Tuttle, Jr., T. R.; Golden, S. *J. Phys. Chem.* **1991**, *95*, 5725.
(48) Hameka, H. F.; Robinson, G. W.; Marsden, C. J. *J. Phys. Chem.* **1987**, *91*, 3150.
(49) Barker, G. C.; Fowles, P.; Sammon, D. C.; Stringer, B. *Trans. Faraday Soc.* **1970**, *66*, 1498.
(50) Marcus, R. A. *Discuss. Faraday Soc.* **1960**, *29*, 129.
(51) Marcus, R. A.; Sutin, N. *Biochem. Biophys. Acta* **1985**, *811*, 265.
(52) Han, P.; Bartels, D. M. *J. Phys. Chem.* **1992**, *96*, 4899.
(53) Debye, P. *Trans. Electrochem. Soc.* **1942**, *82*, 265.
(54) Quist, A. S.; Marshall, W. L. *J. Phys. Chem.* **1965**, *69*, 2984.
(55) Schmidt, K. H.; Han, P.; Bartels, D. M. *J. Phys. Chem.* **1992**, *96*, 199.
(56) Sutin, N. *Prog. Inorg. Chem.* **1983**, *30*, 441.
(57) Scatchard, G. *Chem. Rev.* **1932**, *10*, 229.
(58) Barat, F.; Gilles, L.; Hickel, B.; Lesigne, B. *J. Phys. Chem.* **1973**, *77*, 1711.
(59) Maham, Y.; Freeman, G. R. *J. Phys. Chem.* **1988**, *92*, 1506.
(60) $\Delta H°(1)$ is estimated to increase by 2.7 kcal mol^{-1} in going from 25 to 100 °C.
(61) Christensen, H.; Sehested, K. *J. Phys. Chem.* **1986**, *90*, 186.
(62) The estimation is based on extrapolation of k_2 in ref 21 and k_{-2} in ref 20. Linear Arrhenius plots were assumed for k_2/(density of water) and k_{-2} in the molar unit.
(63) Hartig, K. J.; Getoff, N. *J. Photochem.* **1982**, *18*, 29.
(64) $k(H + H_2O \rightarrow H_2 + OH)$ is estimated to be about 2×10^{-3} s^{-1} at 25 °C, but it may increase to about 1×10^4 s^{-1} at 250 °C.